Supporting Information

Synthesis of Metal-Organic Framework Cu-Mi-UiO-66-based Fluorescent Nanoprobe for Simultaneous Sensing and Intracellular Imaging of GSH and ATP

Yun Liu[a#], *Shuqi Xia*[a#], *Meng Xiao*[a], *Mo Yang*[d], *Mengsu Yang*[c], *Changqing Yi*[a,b*]

a. Key Laboratory of Sensing Technology and Biomedical Instruments (Guangdong Province), School of Biomedical Engineering, Sun Yat-Sen University, Guangzhou 510275, China

b. Research Institute of Sun Yat-Sen University in Shenzhen, Shenzhen 518057, China.

c. Department of Biomedical Sciences, City University of Hong Kong, Hong Kong SAR, China.

d. Department of Biomedical Engineering, The Hong Kong Polytechnic University, Hong Kong SAR, China.

[#] These authors contributed equally to this work.

[*] Authors to whom any correspondence should be addressed.

Email: yichq@mail.sysu.edu.cn

Table of contents

Reagents and instrumentation

Dimethylaminoterephthalate, 1-butyl-3-methylImidazolium hexafluorophosphate ([BMIm][PF_6]), dichloromethane (CH_2Cl_2), tetrahydrofuran (THF), ethyl alcohol, methyl alcohol (MEOH), and sodium hydroxide (NaOH) were obtained from Macklin Biochemical Co. (Shanghai, China). Maleic anhydride, copper(ii) nitrate hydrate ($Cu(NO_3)_2 \cdot 3H_2O$), zirconium tetrachloride ($ZrCl_4$), N,N-dimethylformamide (DMF), glutathione (GSH), thiazolyl blue (MTT), methyl sulfoxide (DMSO), and oligomycin were obtained from Aladdin chemical Co. (Shanghai, China). Ether was purchased from Guangzhou Chemical Reagent Factory (Guangzhou, China). Adenosine triphosphate (ATP) was purchased from Solarbio Science & Technology Co. Ltd (Beijing, China). Dulbecco's Modified Eagle Medium (DMEM), fetal bovine serum (FBS), trypsin and penicillin-streptomycin (double antibody) were obtained from Gibco BRL (Grand Island, New York, USA). Cell lysis buffer (RIPA) was purchased from Biosharp (Hefei, China). SYTO Green was purchased from KeyGEN Bio-Tech Co., Ltd (Nanjing, China). N-Ethylmaleimide (NEM) was purchased from OKY Bio-Tech Co. (Beijing, China). α-lipoic acid (ALA) and etoposide were purchased from Acmec Biochemical Co., Ltd (Shanghai, China). The ATP aptamer modified with fluorescent dye Cy5 (5’-Cy5-ACCTGGGGGAGTATTGCGGAGGAAGGT-3’) was purchased from Sangon Biotech Co., Ltd (Shanghai, China). Commercial GSH and ATP standard testing kits were purchased from Boxbio Technology Co. (Beijing, China). Deionized (DI) water was obtained from a Millipore water purification system.

The nuclear magnetic resonance hydrogen spectrum (^{1}HNMR) was measured using an AVANCE IIIT 600HD 600 MHz spectrometer (Bruker BioSpin, Switzerland). The hydrodynamic diameters and zeta potential were determined using a MS2000 Zetasizer Nano-ZS90 (Malvern, UK). Transmission electron microscopy (TEM) images were obtained using a JEM-1400 electron microscope (JEOL, Japan), and scanning electron microscopy (SEM) images were obtained using a Sigma 300 electron microscope (Carl Zeiss, Germany). The porosity was measured by an APSP 2460 aperture analyzer (Micromeritics, USA). The ultraviolet-visible (UV-vis) absorption spectra were measured on a DU-730 ultraviolet/visible spectrophotometer (Beckman, USA). X-ray diffraction (XRD) patterns were acquired on an Empyrean XRD system (PANalytical, Netherlands). X-ray photoelectron spectroscopy (XPS) patterns were acquired on an ESCALAB 250 X-ray photoelectron spectrometer (THERMOP-VG scientific, USA). Fluorescence spectra were measured on a Spectrofluorometer FS5 (Edinburgh, Scotland). Confocal microscope images were observed using a confocal laser scanning microscope TCS SP5 (Leica, Germany).

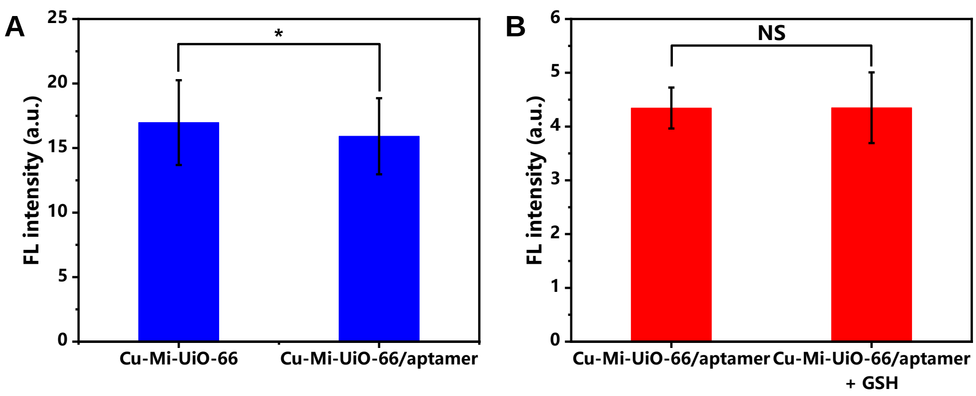

Fig. S1. (A) Fluorescence intensity at 455 nm of Cu-Mi-UiO-66 and Cu-Mi-UiO-66/aptamer, (B) Fluorescence intensity at 670 nm of Cu-Mi-UiO-66/aptamer without or with GSH (Paired sample *t* test; NS: no significant difference, $p > 0.05$; *: $0.05 < p < 0.01$; **: $p < 0.01$).

Synthesis and characterization of ligand H_2L1

The synthesis of maleimide functional ligand H_2L1 was characterized by ^{1}HNMR and mass spectrometry (MS). First of all, as shown in **Fig. S2A**, the proton peaks at 3.77 ppm and 3.91 ppm were attributed to 6 methyl H on the ester groups at both ends of the intermediate ester, while the proton peak at 7.27 ppm was attributed to two H on the maleimide groups, confirming the successful synthesis of the intermediate ester. In **Fig. S2B**, the proton peak of methyl hydrogen at 3 ~ 4 ppm disappeared, and a carboxyl H peak after ester hydrolysis appeared at 11.27 ppm, indicating the successful synthesis of the ligand H_2L1 containing carboxyl and maleimide groups. In terms of MS results, **Fig. S3A** showed the characteristic peak (289.059 m/z) attributed to the intermediate ester. As shown in **Fig. S3B**, the peak at 278.033 m/z was assigned to the characteristic peak after the ligand H_2L1 had removed the proton and added water. Since the maleimide group was prone to hydrolysis under alkaline conditions, the characteristic peak of amino terephthalic acid, a byproduct of the hydrolysis reaction, appeared at 180.030 m/z. In conclusion, the ligand H_2L1 was successfully synthesized through the two-step reaction.

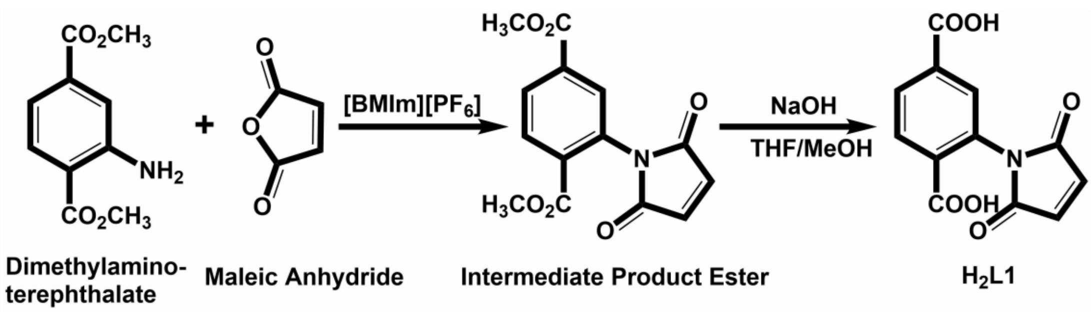

Scheme S1. The synthetic route of H_2L1 ligand.

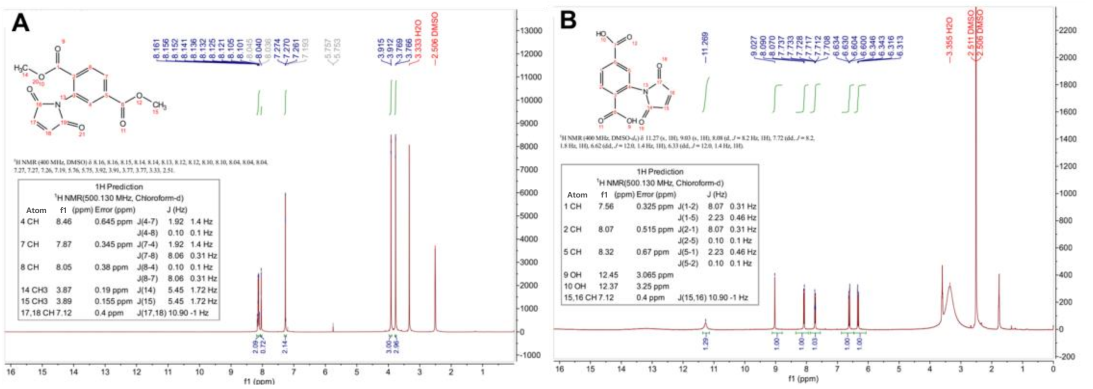

Fig. S2. ^{1}H NMR spectra of the intermediate ester (A) and the final product H_2L1 ligand (B).

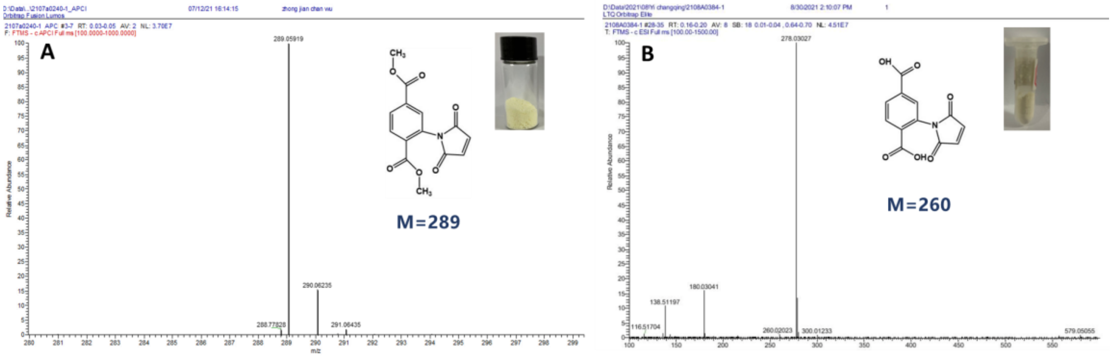

Fig. S3. MS spectra of the intermediate ester (A) and the final product H_2L1 ligand (B).

Synthesis and characterization of NMOF-based nanoprobes

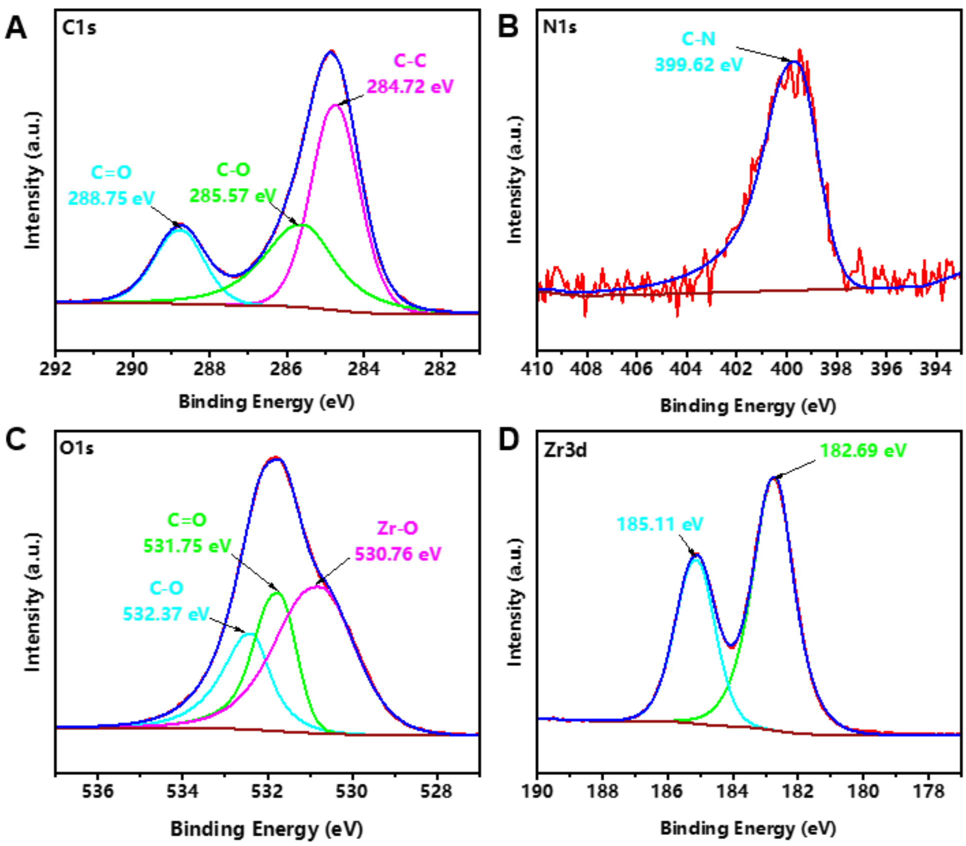

Fig. S4. Peak-differentiation-imitating analysis C1s (A), N1s (B), O1s (C) and Zr3d (D) of the deconvoluted XPS spectra of Mi-UiO-66.

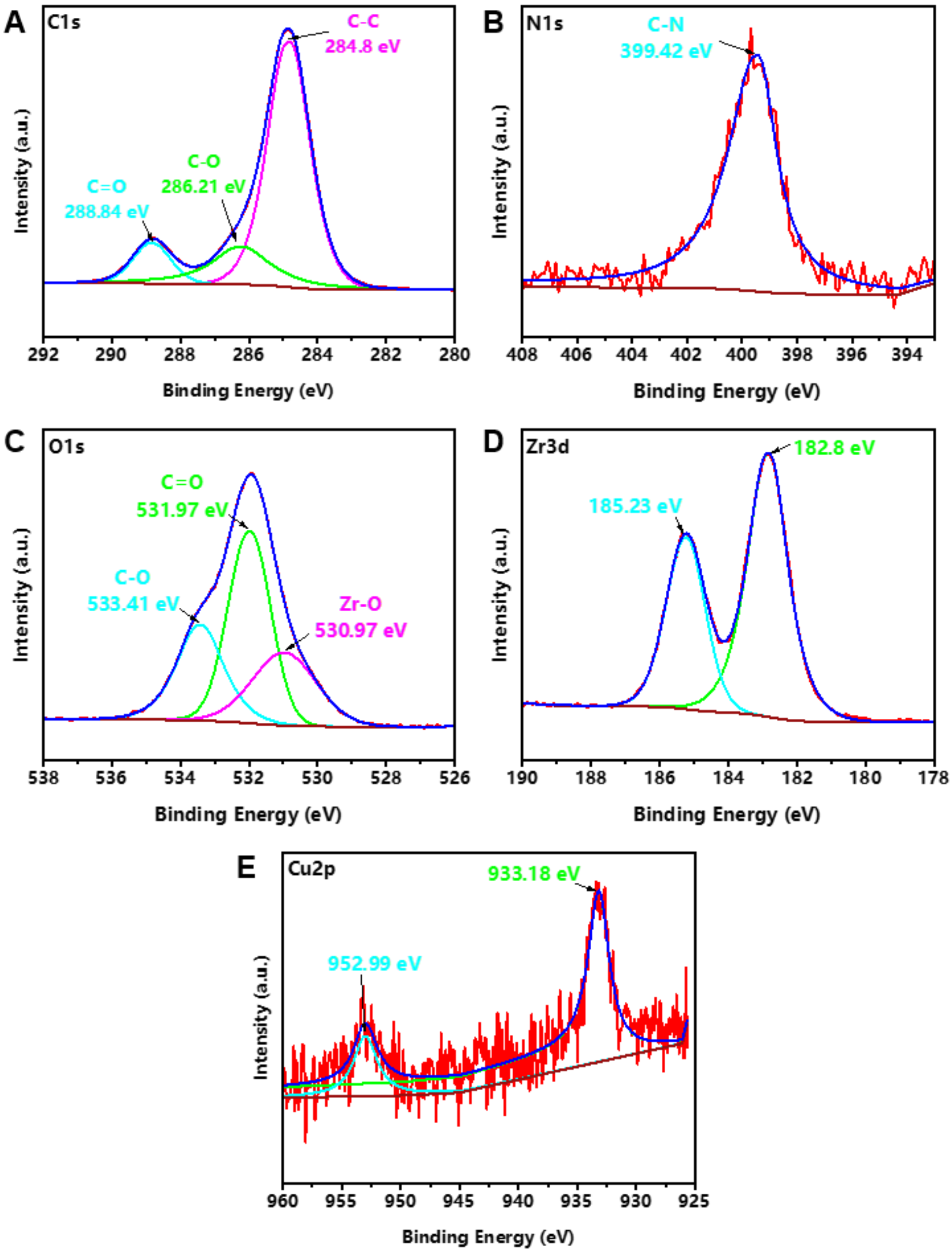

Fig. S5. Peak-differentiation-imitating analysis C1s (A), N1s (B), O1s (C), Zr3d (D) and Cu2p (E) of the deconvoluted XPS spectra of Cu-Mi-UiO-66.

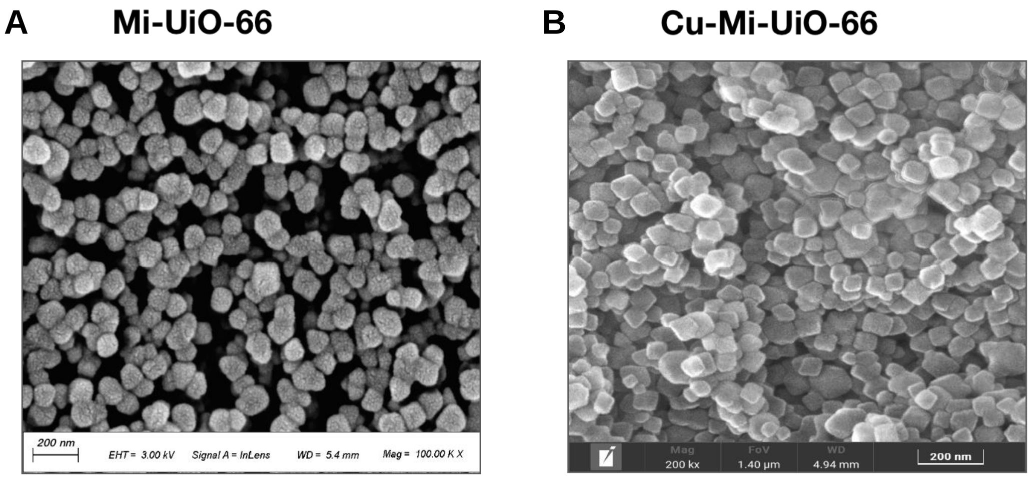

Fig. S6. SEM images of Mi-UiO-66 (A) and Cu-Mi-UiO-66 (B).

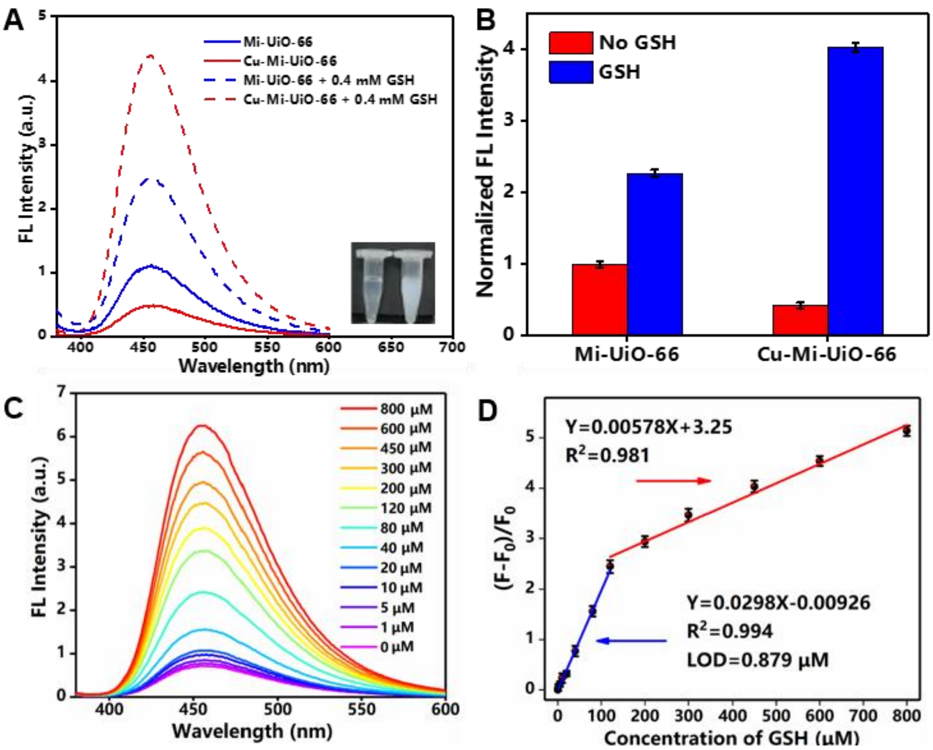

Fig. S7. (A-B) Fluorescence spectra (A) and fluorescence intensity at 455 nm (B) of Mi-UiO-66 and Cu-Mi-UiO-66 in the absence and presence of 0.4 mM GSH. (C) Fluorescence spectra of Cu-Mi-UiO-66 with different concentrations of GSH (0 - 800 μM). (D) Linear relationship between ΔF_{455} and GSH concentrations.

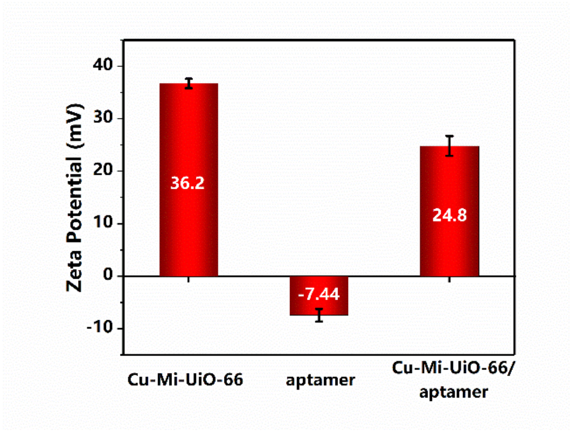

Fig. S8. Zeta potential of Cu-Mi-UiO-66, aptamer and Cu-Mi-UiO-66/aptamer.

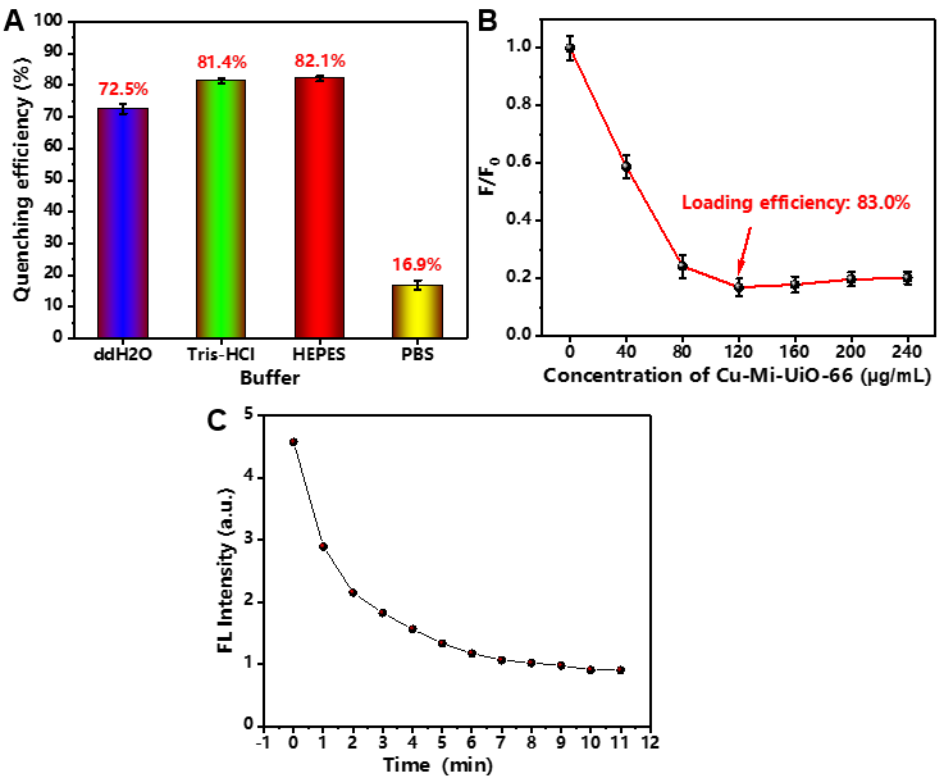

Fig. S9. (A) Decrease in fluorescence intensity (λ_{em} = 670 nm) of solution containing 100 nM Cy5-labeled aptamer after being reacted with Cu-Mi-UiO-66 in different buffer solutions. (B) Decrease in fluorescence intensity (λ_{em} = 670 nm) of solution containing 100 nM Cy5-labeled aptamer after being reacted with different concentrations of Cu-Mi-UiO-66. (C) Time-dependent fluorescence intensity changes of solution containing 100 nM Cy5-labeled aptamer after being reacted with 120 μg/mL Cu-Mi-UiO-66 in HEPES buffer.

Table S1. Comparison of different methods for the determination of GSH

Target	Detection method	Linear range (μM)	LOD (μM)	Reference
GSH	FL	5-450	2.17	This work
	EC	0.1-5	0.133	[1]
	FL	0.01-6	0.0015	[2]
	Colorimetric	0.02-3, 3-50	0.02	[3]
	Colorimetric	10-400	1.88	[4]
	Colorimetric	5-100	0.33	[5]
	PL	10-50, 50-200	0.62	[5]

Note: FL, fluorescence; EC, electrochemical; PL, persistent luminescence.

Table S2. Comparison of different methods for the determination of ATP

Target	Detection method	Linear range (μM)	LOD (μM)	Reference
ATP	FL	1-50, 50-800	0.635	This work
	FL	10-200	4.24	[6]
	CL	2-2000	0.0843	[7]
	FL	9000-24000	3	[8]
	FL	0.78-50	4.75	[9]
	FL	0-200	0.55	[10]
	FL	1-200	0.4	[11]

Note: CL, chemiluminescence.

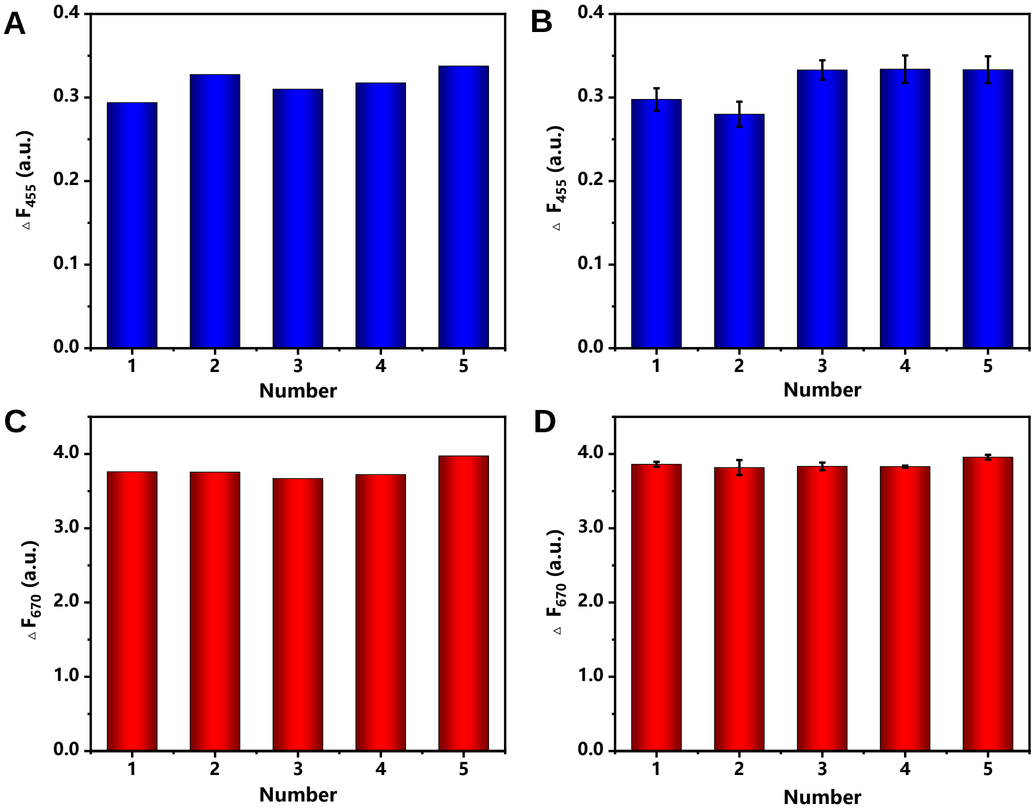

Fig. S10. (A, B) Intra-assay (A) and inter-assay (B) results for the determination of GSH using Cu-Mi-UiO-66/aptamer. (C, D) Intra-assay (C) and inter-assay (D) results for the determination of ATP using Cu-Mi-UiO-66/aptamer.

Quantitation of GSH and ATP in cell lysate

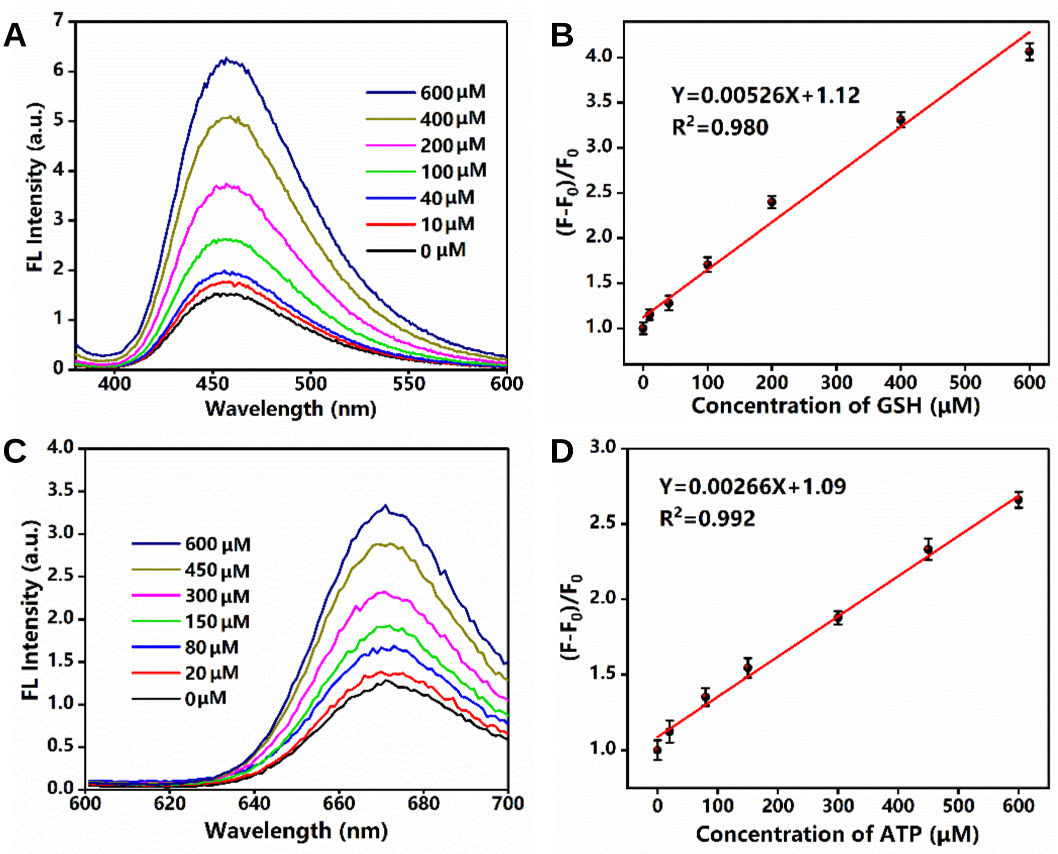

Fig. S11. The fluorescence spectra of Cu-Mi-MOF/aptamer in response to different concentrations of GSH (A) and ATP (C) in cell lysate. Linear plots of fluorescence quenching efficiency (ΔF_{455} (B) or ΔF_{670} (D)) of Cu-MOFs/aptamer as a function of the GSH concentration (B) and the ATP concentration (D).

Fluorescence imaging of intracellular GSH and ATP

Cytotoxicity Assay. Once the cells had reached a suitable confluency, they were seeded into 96-well plates at a density of 5 × 10^3 cells/well. The outermost wells were filled with 100 μL of PBS to prevent liquid evaporation. The plates were then incubated overnight to allow the cells to adhere to the wells. FBS-free DMEM medium was used to prepare different concentrations of Mi-UiO-66, Cu-Mi-UiO-66, and Cu-Mi-UiO-66/aptamer solutions (0, 40, 80, 120, 160, 200, 250, 300 μg/mL, 100 μL), which were added to the wells to replace the original culture medium. The plates were then incubated for another 24 h. Afterward, the plates were rinsed, and 100 μL of medium and 20 μL of MTT-PBS solution (5 mg/mL) were added to each well. The plates were further incubated for 4 h before being rinsed again. Finally, 150 μL DMSO was added to each culture well and shaken at a low speed and away from light for 15 min to promote complete dissolution of the blue-purple formazan crystals. The absorbance (A) of each well in the 96-well plate was measured at 570 nm using a multifunctional enzyme marker. The cytocompatibility of the control group (without fluorescence probe) was set to 100 %, and only the wells containing PBS were included as the blank group. The formula for calculating the cell survival rate is as follows:

$$cell\ survival\ rate = \frac{A_{experimental} - A_{blank}}{A_{control} - A_{blank}} \times 100\ \%$$

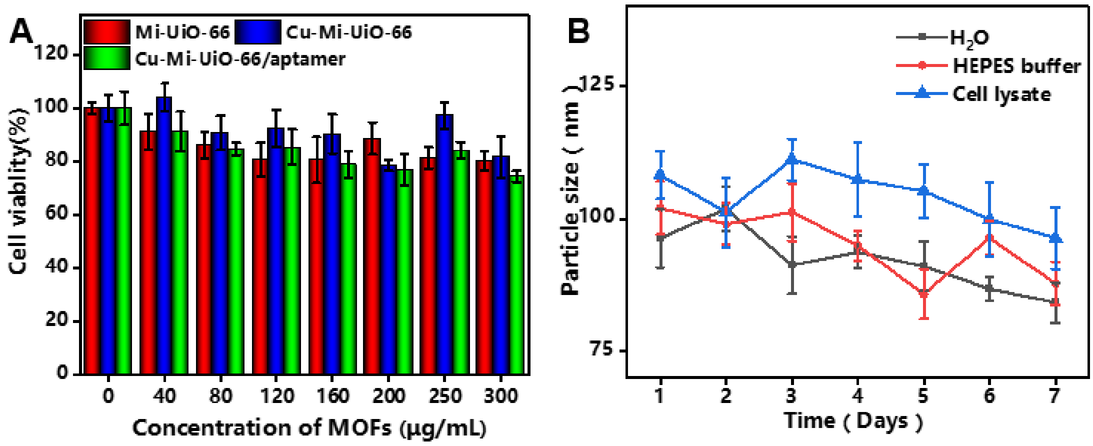

Fig. S12. (A) Viability of HepG2 cells upon treatment with Mi-UiO-66, Cu-Mi-UiO-66 and Cu-Mi-UiO-66/aptamer for 24 h. (B) Particle size of Cu-Mi-UiO-66/aptamer in ddH_2O, HEPES buffer and cell lysate as a function of storage days.

References

1. S. M. Lee, H. Kim, P. Li and H. G. Park, *Biosens. Bioelectron.*, 2024, **250**, 116019.
2. L. Yang, N. Jiang, Z. Zhang, X. Zhang, H. Wu, Z. Li and Z. Zhou, *Talanta*, 2024, **270**, 125652.
3. T. Zhang, N. Lu, M. Zhang, R. Zhang, H. Jiang, C. Wang and D. Xing, *ACS Appl. Nano Mater.*, 2024, **7**, 756-765.
4. X. Cheng, X. Zhou, Z. Zheng and Q. Kuang, *Chem. Eng. J.*, 2022, **430**, 133079.
5. X. Chen, H. Zhang, X. Liang and L. Li, *Sens. Actuat. B Chem.*, 2024, **403**, 135200.
6. X. Shi, H. Xu, Y. Wu, Y. Zhao, H. Meng, Z. Li and L. Qu, *J. Anal. Test.*, 2021, **5**, 165-173.
7. H. Chen, Y. Feng, F. Liu, C. Tan, N. Xu, Y. Jiang and Y. Tan, *Biosens. Bioelectron.*, 2024, **247**, 134249.
8. Y. Li, Z. Meng, Y. Liu and B. Zhang, *RSC Adv.*, 2024, **14**, 5594-5599.
9. Y. Xiong, J. Zhang, Z. Yang, Q. Mou, Y. Ma, Y. Xiong and Y. Lu, *J. Am. Chem. Soc.*, 2020, **142**, 207-213.
10. L. Kaisu, Y. Songlin, S. Wu, Z. Ying, L. Wang, A. Potapov, X. Yu, Y. Sun, N. Sun and M. Zhu, *ACS Appl. Mater. Inter.*, 2024, **16**, 5129-5137.
11. L. Peng, J. Zhou, G. Liu, L. Yin, S. Ren, S. Man and L. Ma, *Sens. Actuat. B Chem.*, 2020, **320**, 128164.